JOURNAL OF MATERIALS SCIENCE 27 (1992) 1449–1456

Cyclic stress–strain curves at finite strains under high pressures in crystalline polymers

M. KITAGAWA, J. QUI, K. NISHIDA, T. YONEYAMA
Department of Mechanical Engineering, Faculty of Technology, Kanazawa University, Kodatsuno 2-40-20, Kanazawa, Japan

The cyclic torsional stress–strain behaviour for crystalline polymers of polyethylene (PE), polypropylene (PP) and polyoxymethylene (POM) was investigated at finite strain amplitude under hydrostatic pressure up to 2000 kgf cm^{-2}. The following features for the cyclic stress–strain curves were indicated. (1) Two types of cyclic stress–strain curve were observed: one was a PE type where the present hysteresis loop was not so affected by the strain histories, and the other was a PP type where the hysteresis loop was greatly affected by the previous maximum strain. (2) In the pressure ranges tested, the shape of the cyclic stress–strain curves for the polymers used was not essentially altered by the hydrostatic pressure. (3) The stress–strain curves after the first strain reversal showed an unusual shape which has not been observed for metals. (4) The decrease in cyclic softening caused by the stress amplitude with increasing number of cycles at a constant strain amplitude test occurred irrespective of the hydrostatic pressure. (5) The stress–strain behaviour at a partly reversed cyclic loading was different from that expected at a fully reversed cyclic loading.

1. Introduction

Although a great effort has been made to introduce a nonlinearity in the linear theory of viscoelasticity, the nonlinear behaviour at finite strains are less understood because of the many complexities peculiar to polymer solids. In previous papers, the stress–strain curves under uniaxial compression [1], torsion [2, 3] and combined tension–torsion [4, 5] were investigated experimentally to point out some important facts required for constructing the constitutive equation for time-sensitive polymers.

One of the important factors influencing the stress–strain behaviour of polymers is hydrostatic pressure. The pressure-dependent behaviour of polymers has been widely investigated by many researchers [6–10] since the pioneering work of Rabinowitz *et al.* [11]. Most of these tests were executed at a constant strain rate under a monotonic strain increase without strain reversal. These data show that the hydrostatic pressure results in an increase in the magnitude of elastic modulus and yield stress for most of the polymers tested. But less attention has been paid to the shape of the stress–strain curve including strain reversal and cyclic loading. In order to discuss a constitutive equation for pressure-sensitive materials, a noticeable influence of the hydrostatic pressure on the exact stress–strain curves must be studied.

In addition, high polymer solids will be used increasingly in future for operations in the deep sea. Fatigue tests under high hydrostatic pressure will become necessary. For these purposes, the effect of pressure on the cyclic torsional stress–strain curves for crystalline polymers of polyethylene (PE), polypropylene (PP) and polyoxymethylene (POM) were investigated.

2. Experimental procedure

The materials used were commercial grades of PE, PP and POM rods with diameter 20 mm. Hollow cylindrical specimens with outer radius $r_o = 4$ mm, inner radius $r_i = 3$ mm and gauge length $L = 12$ mm were machined from these rods. This shape of specimen did not cause shear buckling up to a shear strain of about 0.3.

A home-made high-pressure torsion apparatus was used in this experiment. Torque, T, was measured by a torque meter set in a pressure chamber, which was developed by our laboratory. The angular displacement, θ, was measured by a potentiometer circuit, and the relationship between θ and the twist angle, ϕ, over the specimen gauge length, L, was determined experimentally in air as a proportionality function of $\phi = f\theta$. The strain, γ, averaged over the specimen gauge length was calculated from

$$\gamma = (r/L)\phi = f(r/L)\theta \quad (1)$$

where $r = (r_o + r_i)/2$ is the mean radius of the specimen and f is a proportionality constant between ϕ and θ. The factor f is slightly different for every material. The value of f may be higher under high pressure than in air. But this is not considered here.

0022–2461

The shear stress, τ, averaged over the cross-section was calculated from

$$\tau = T/[\pi r(r_o^2 - r_i^2)]. \quad (2)$$

These signals were recorded on a microcomputer.

The grips for fixing a specimen in the pressure chamber were specially devised so that the hydrostatic pressure did not act along the longitudinal axis of specimen due to the friction between the grips and the specimen. The details are shown schematically in Fig. 1.

When a predetermined pressure is applied to the specimen mounted in the equipment through a pressure medium (turbine oil), the temperature of the specimen in the pressure vessel rises so that the stress–strain curve obtained may depart from an expected one. When the hydrostatic pressure increases up to 1500 kgf cm^{-2} in an abrupt manner, the temperature rise of the specimen surface amounts to about 10 °C. Hence, after the specimen was left at the predetermined pressure for more than 30 min and the temperature decreased to the test temperature (25 °C), the specimen was cyclically twisted at a constant strain rate. The maximum variation of pressure during the test was within 50 kgf cm^{-2}. The temperature rise measured by a thermocouple during cyclic torsion was less than 1 °C. Under these tests conditions, crazing was not observed. Hence, the stress–strain curves obtained in this experiment are supposed to be intrinsic. The cyclic tests were conducted at a triangular wave form under a strain-controlled condition. The strain histories tested here are schematically illustrated in Table I.

3. Results and discussion

3.1. Fully reversed cyclic loading

Figs 2–4 illustrate the fully reversed cyclic stress–strain (SS) behaviour for a strain amplitude of $\Delta\gamma/2 = 0.13$ at a strain rate of 1.8×10^{-3} s^{-1} in PE, PP and POM (see Table Ia). The strain amplitude $\Delta\gamma/2 = 0.13$ corresponds to an equivalent tensile strain of $\Delta\varepsilon_{eq.}/2 = (\Delta\gamma/2)3^{-1/2} = 0.075$. This amplitude is chosen so that the torsional loops can be compared with the tensile data in air which are not reported here. The results obtained at a strain rate of 1.8×10^{-2} s^{-1} were similar to those at 1.8×10^{-3} s^{-1} except for the magnitude of the flow stress. To facilitate the interpretation of the results, the numbers 0, 1, 2, etc., are marked on the SS curve as described in Fig. 3. The numeral denotes the number of cycles, and the letters a and b indicate the initial and the reversed torsional direction, respectively. Curve 0 denotes the initial one up to the first strain reversal point.

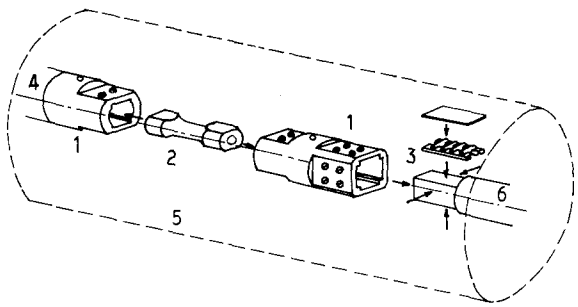

Figure 1 Schematic illustration of the structure of the grips. The grips consists of two pairs of roller bearings so that the friction between the specimen and the grip will be as small as possible. The parts shown in the figure were set in a pressure vessel denoted by the dotted line. 1, grip; 2, specimen; 3, roller bearings; 4, load cell; 5, pressure vessel; 6, to mortar.

Many interesting features required for constructing the constitutive equation are noted. (1) As mentioned already, there is a monotonic increase in the initial slope (elastic modulus) and the initial flow stress on the SS curve (0) with increasing pressure. (2) For the materials tested, the shape of the hysteresis loops at the high hydrostatic pressures is similar to that at atmospheric pressure. (3) For the crystalline polymers used here, the transition from elastic behaviour to shear yielding is smooth with no sharp stress drop. In particular, on the SS curves except for the initial one, the definition of yielding becomes vague because of their shape. Hence, the distinction between elastic strain and plastic strain is difficult. (4) The tangential slope of the SS curve just after strain reversal is larger than the initial one at the origin. (5) The shape of Curve 0 is very different from all subsequent ones such as 1a, 1b, 2a etc. The similarity of Curve 0 to the subsequent ones is not realized. (6) The anomalous behaviour that the SS curve marked 1b becomes convex upwards in the neighbourhood of P in Fig. 3 is observed in Curve 1b. (7) As the cyclic number increases, the absolute values of both the maximum stress and the minimum stress decreases gradually (cyclic softening) and the SS curve tends to reach a steady state in which the loop is traced over and the hysteresis loop becomes symmetric with respect to the origin.

Features 3–7 seem independent of applied pressure and materials tested. The results mentioned above are very different from the results observed in most metals. Fact 3, above, may show that a plastic potential theory, where the plastic strain increment is distinguished from the total strain increment, is not necessarily suitable for strongly time-sensitive materials because of the vagueness of the definition of yielding. It may be very important for the construction of the constitutive law to investigate the physical mechanisms which govern these curious facts mentioned above.

Figs 5–7 show the variation in the maximum and minimum stresses with the number of cycles under various pressures. The maximum stress gradually decreases (the cyclic softening) and it approaches a stable value asymptotically, seemingly independent of the hydrostatic pressure. It is noteworthy to point out that the extent of cyclic softening is considerably smaller for PE than for PP and POM.

The results obtained at other strain amplitudes share the common features mentioned above.

3.2. Partly reversed cyclic loading

Figs 8 and 9 denote the partly reversed hysteresis loops in PE and POM. The strain path is schematically illustrated in Table Ib. The specimen was cyclically

TABLE I Schematic illustration of cyclic wave forms

(a) Fully reversed	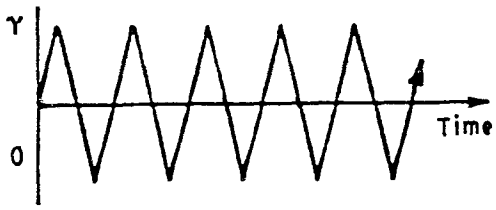	$\Delta\gamma = 0.26$
(b) Partly reversed	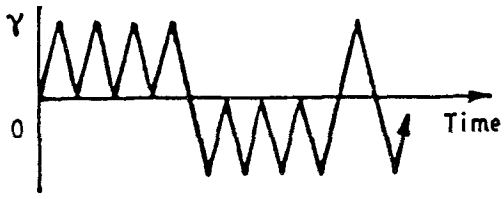	$\Delta\gamma = 0.13$ ↓ $\Delta\gamma = 0.13$ ↓ $\Delta\gamma = 0.26$
(c) Increasing amplitude	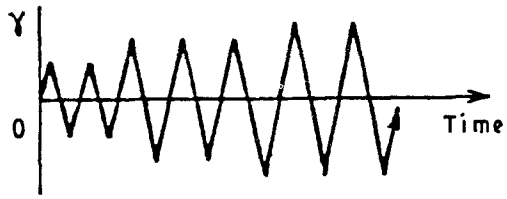	$\Delta\gamma = 0.08$ ↓ $\Delta\gamma = 0.12$ ↓ $\Delta\gamma = 0.17$ ↓ $\Delta\gamma = 0.22$
(d) Decreasing amplitude	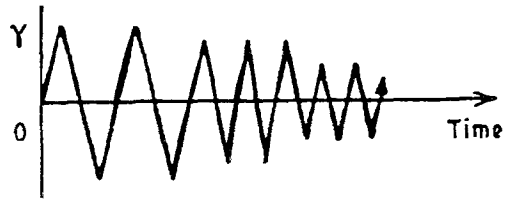	$\Delta\gamma = 0.26$ ↓ $\Delta\gamma = 0.17$ ↓ $\Delta\gamma = 0.08$
(e) Increasing and decreasing amplitude	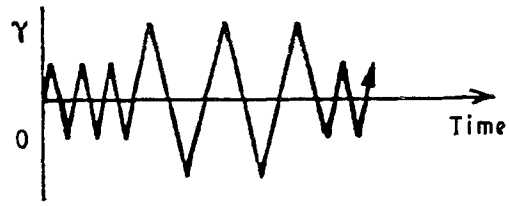	$\Delta\gamma = 0.17$ ↓ $\Delta\gamma = 0.26$ ↓ $\Delta\gamma = 0.17$

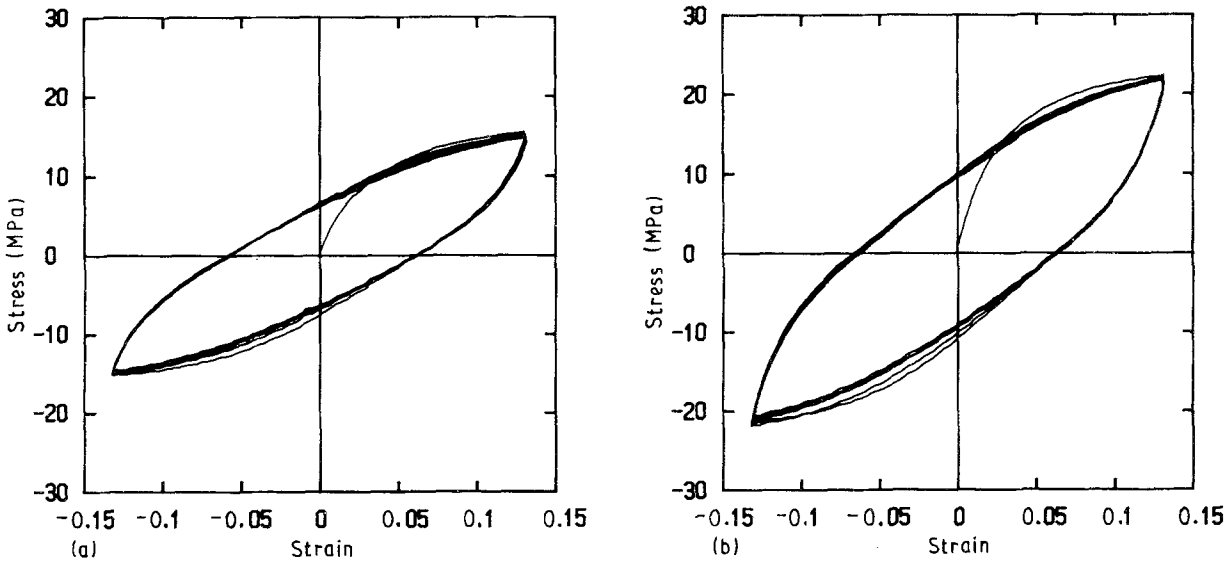

Figure 2 Hysteresis loops at a strain amplitude of 0.13 at a strain rate of $1.8 \times 10^{-3}\ s^{-1}$ in a fully reversed cyclic loading under hydrostatic pressure of (a) 1 kgf cm^{-2} and (b) 1000 kgf cm^{-2} in PE.

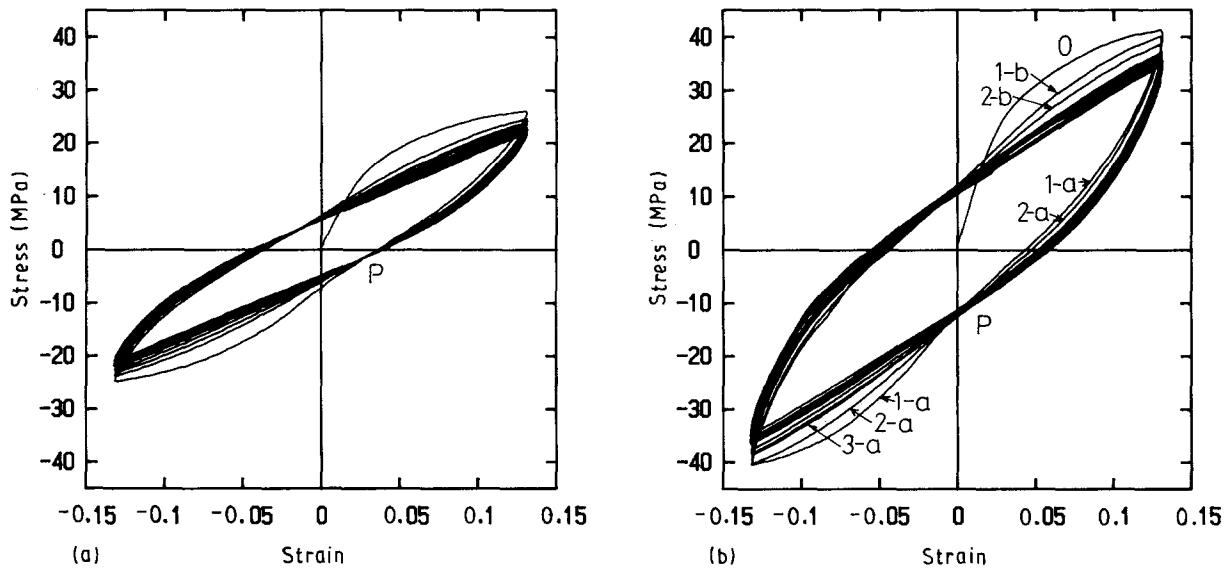

Figure 3 Hysteresis loops at a strain amplitude of 0.13 at a strain rate of $1.8 \times 10^{-3}\ s^{-1}$ in a fully reversed cyclic loading under hydrostatic pressure of (a) 1 kgf cm^{-2} and (b) 1000 kgf cm^{-2} in PP.

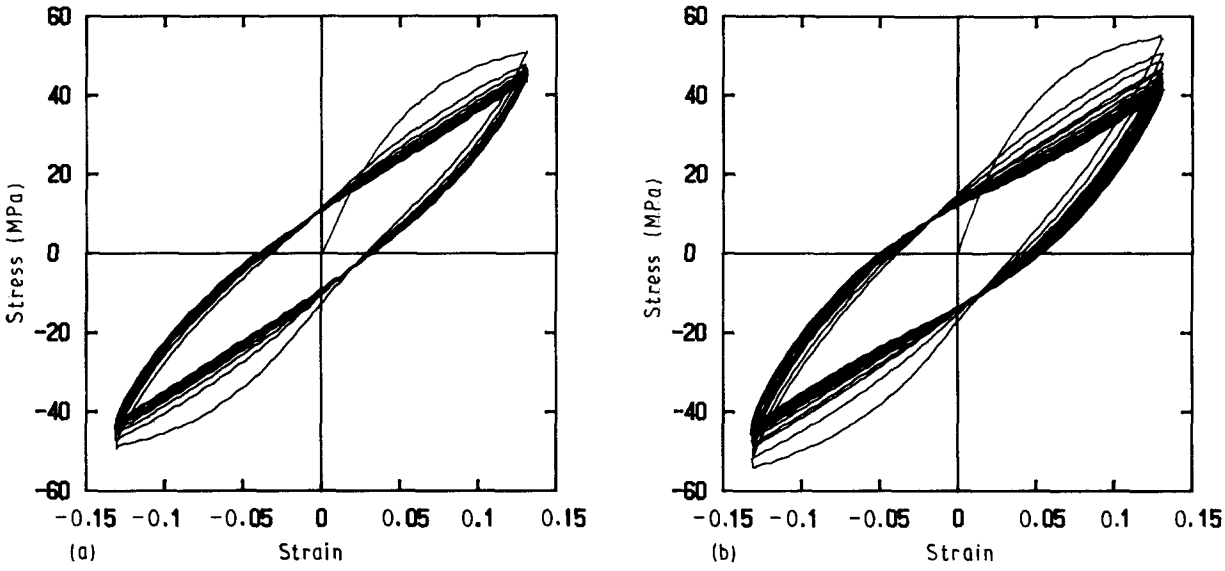

Figure 4 Hystersis loops at a strain amplitude of 0.13 at a strain rate of $1.8 \times 10^{-3}\ s^{-1}$ in a fully reversed cyclic loading under hydrostatic pressure of (a) 1 kgf cm^{-2} and (b) 1000 kgf cm^{-2} in POM.

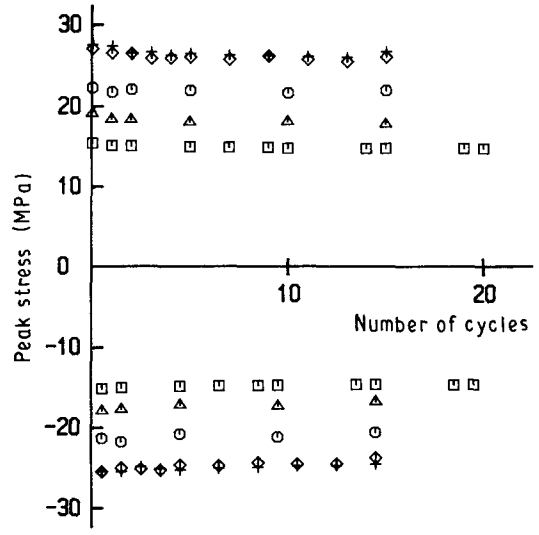

Figure 5 Variation of the maximum and minimum stress in one cycle with the number of cycles at a strain amplitude of 0.13 under various pressures (□) 1 kgf cm^{-2}, (△) 500 kgf cm^{-2}, (○) 1000 kgf cm^{-2}, (◇) 1500 kgf cm^{-2}, (+) 1800 kgf cm^{-2}, in PE.

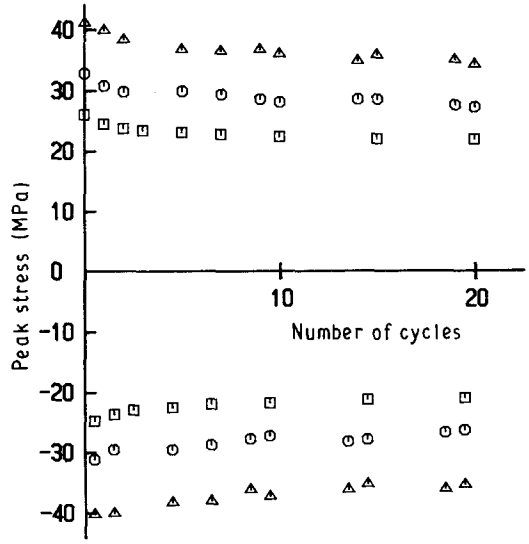

Figure 6 Variation of the maximum and minimum stress in one cycle with the number of cycles at a strain amplitude of 0.13 under various pressures in PP. (□) 1 kgf cm^{-2}, (△) 500 kgf cm^{-2}, (○) 1000 kgf cm^{-2}, (◇) 1500 kgf cm^{-2}, (+) 1800 kgf cm^{-2}, in PE.

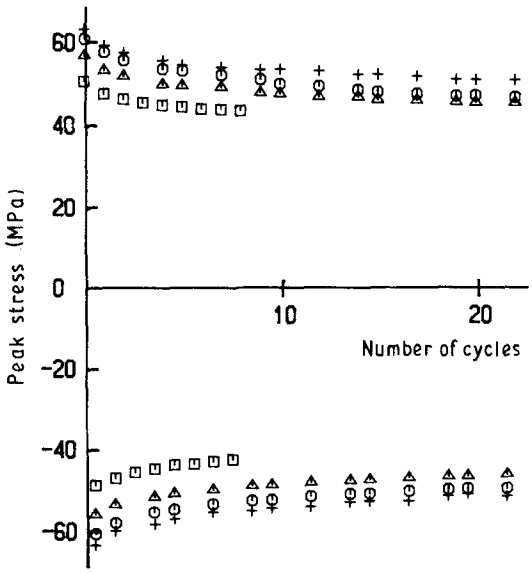

Figure 7 Variation of the maximum and minimum stress in one cycle with the number of cycles at a strain amplitude of 0.13 under various pressures in POM. (□) 1 kgf cm^{-2}, (△) 500 kgf cm^{-2}, (○) 1000 kgf cm^{-2}, (◇) 1500 kgf cm^{-2}, (+) 1800 kgf cm^{-2}, in PE.

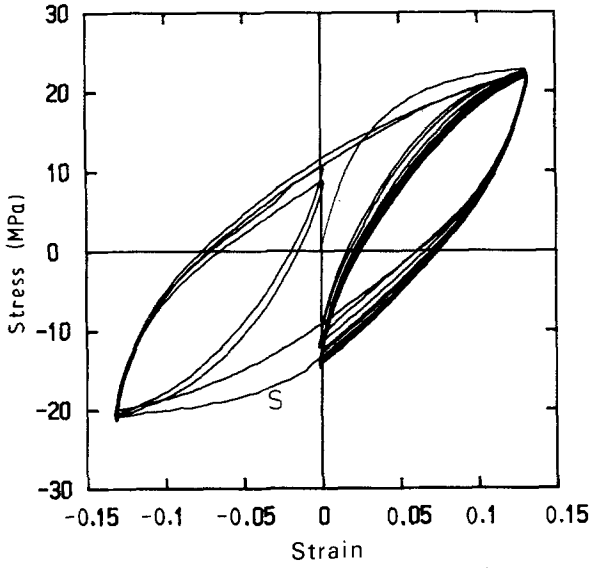

Figure 8 Hysteresis loops at partly reversed cyclic loading at a strain rate of 1.8×10^{-3} s^{-1} under a hydrostatic pressure of 1000 kgf cm^{-2} in PE.

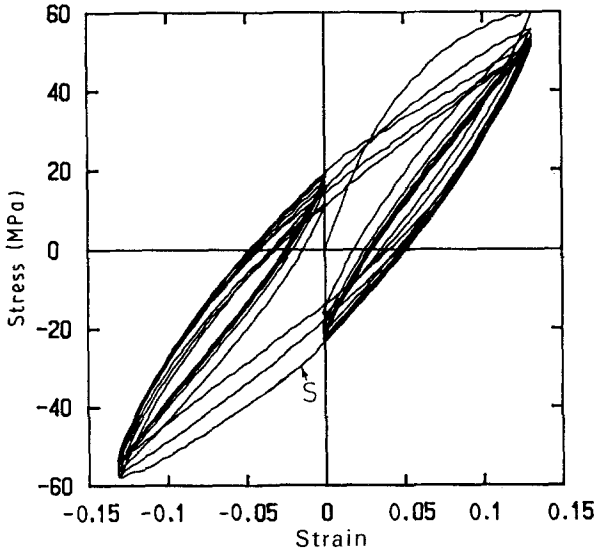

Figure 9 Hysteresis loops at partly reversed cyclic loading at a strain rate of 1.8×10^{-3} s^{-1} under a hydrostatic pressure of 1000 kgf cm^{-2} in POM.

loaded for some cycles in the strain range $\gamma = 0$–0.13 (Step I). Subsequently the strain range changed to $\gamma = 0$ to -0.13 for the next cycles (Step II). Finally, the fully reversed cyclic test was conducted in one cycle in the strain range $\gamma = -0.13$–0.13 (Step III). A similar trend was also observed at atmospheric pressure. The results for PP were similar to those for POM.

At Step I, the stress range (the difference between the maximum and the minimum stresses during one cycle) slightly increases with an increase in the number of cycles. For PE, the stress at the maximum strain is kept nearly constant. Nevertheless, the stress at the minimum strain seems to decrease gradually to a stable value. For POM, except that the maximum stress as well as the minimum stress decreases, the trend is similar to that of PE. This strange behaviour where a slight cyclic hardening appears at the partly reversed loading, seems to be in contrast to the fact that cyclic softening occurs at the fully reversed cyclic loading.

Curve S on the way from Step I and Step II, which is situated at the outer side, is considered. At the last cycle of Step I, the specimen was strained from the maximum strain $\gamma_{max} = 0.13$ to the minimum strain $\gamma_{min} = -0.13$ at a constant strain rate. As the number of cycles at Step I increases, Curve S expands downwards and is located below the curves expected from the fully reversed cyclic test. But the stress at $\gamma_{min} = -0.13$ becomes nearly equal to the stress obtained at the same strain rate in a simple torsion test.

At Step II, the trend of the loops is similar to that at Step I. The hysteresis loops at Step II becomes nearly symmetrical to those at Step I with respect to the origin.

At Step III, the hysteresis loop which expands due to the partly reversed loading is again depressed to the initial hysteresis loop obtained at the fully reversed loading. When subsequently the fully cyclic loading was applied to the specimen for some cycles, the same behaviour as mentioned in Section 3.1 will be repeated as if the specimen forgets the past strain history.

It may be very important for the contruction of the constitutive law to investigate why cyclic softening or hardening occur at fully–partly reversed loading.

3.3. Hysteresis curves at increasing or decreasing strain amplitude

Figs 10–12 represent the hysteresis loops at increasing strain amplitude under 1000 kgf cm^{-2} for PE, PP and POM. Figs 13–15 show the hysteresis loops at decreasing strain amplitudes under 1000 kgf cm^{-2} for PE, PP, and POM. Several loading cycles were performed at each strain amplitude before changing to the subsequent one. The absolute value of the strain rate was kept constant during loading and unloading. The strain histories for both tests are schematically illustrated in Table Ic and d. Because the shape of the hysteresis curves under these conditions is little different between 1 and 1000 kgf cm^{-2}, the loops at 1 kgf cm^{-2} are not shown.

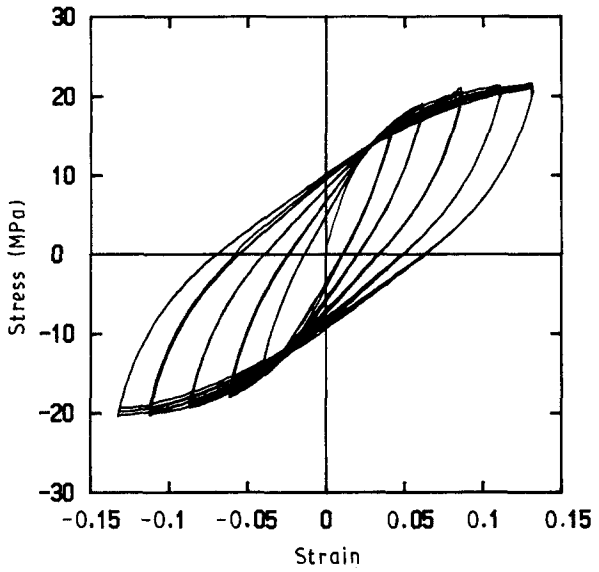

Figure 10 Hysteresis loops at increasing strain amplitude $\Delta\gamma/2 = 0.04 \rightarrow 0.06 \rightarrow 0.085 \rightarrow 0.11 \rightarrow 0.13$ at a strain rate of $1.8 \times 10^{-3}\,s^{-1}$ under a hydrostatic pressure of 1000 kgf cm^{-2} in PE.

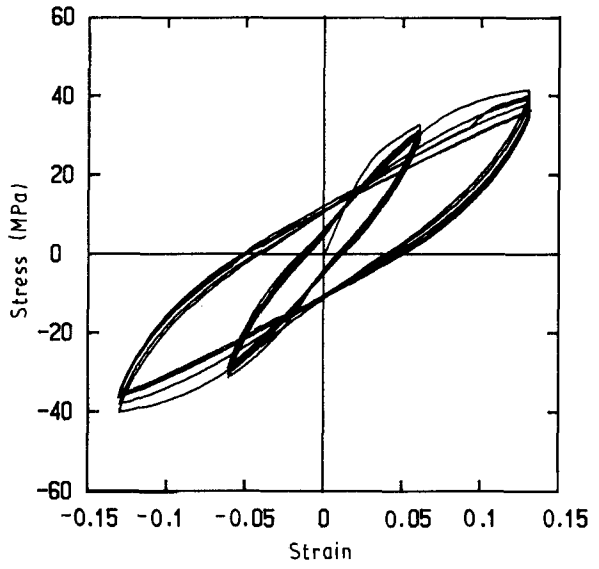

Figure 11 Hysteresis loops at increasing strain amplitude $\Delta\gamma/2 = 0.06 \rightarrow 0.13$ at a strain rate of $1.8 \times 10^{-3}\,s^{-1}$ under a hydrostatic pressure of 1000 kgf cm^{-2} in PP.

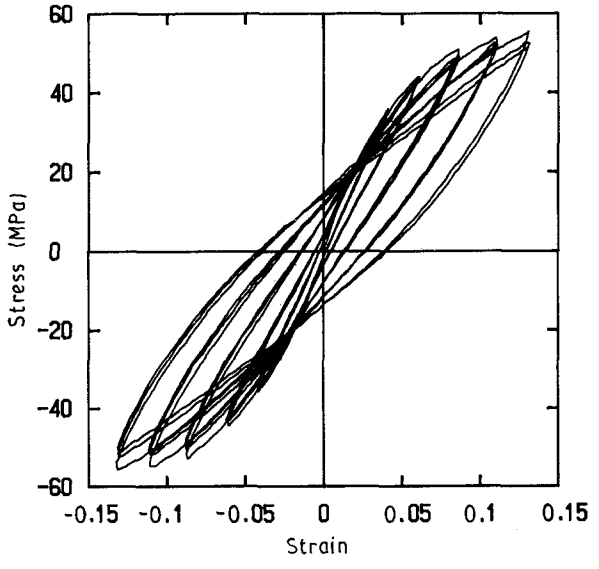

Figure 12 Hysteresis loops at increasing strain amplitude $\Delta\gamma/2 = 0.04 \rightarrow 0.06 \rightarrow 0.085 \rightarrow 0.11 \rightarrow 0.13$ at a strain rate of $1.8 \times 10^{-3}\,s^{-1}$ under a hydrostatic pressure of 1000 kgf cm^{-2} in POM.

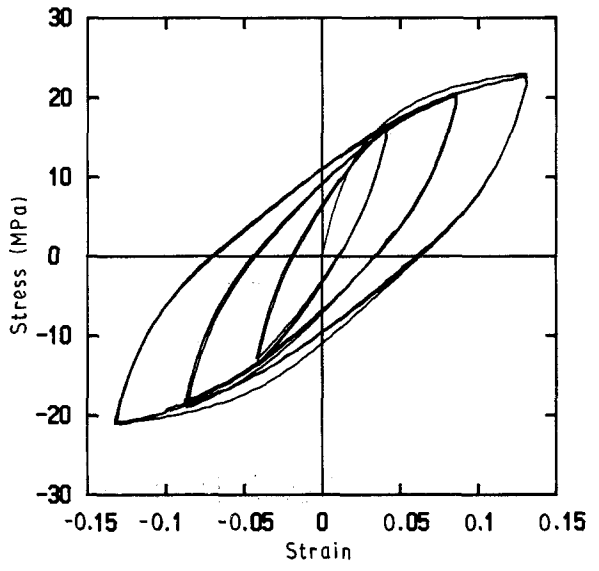

Figure 13 Hysteresis loops at decreasing strain amplitude $\Delta\gamma/2 = 0.13 \rightarrow 0.085 \rightarrow 0.04$ at a strain rate of $1.8 \times 10^{-3}\,s^{-1}$ under a hydrostatic pressure of 1000 kgf cm^{-2} in PE.

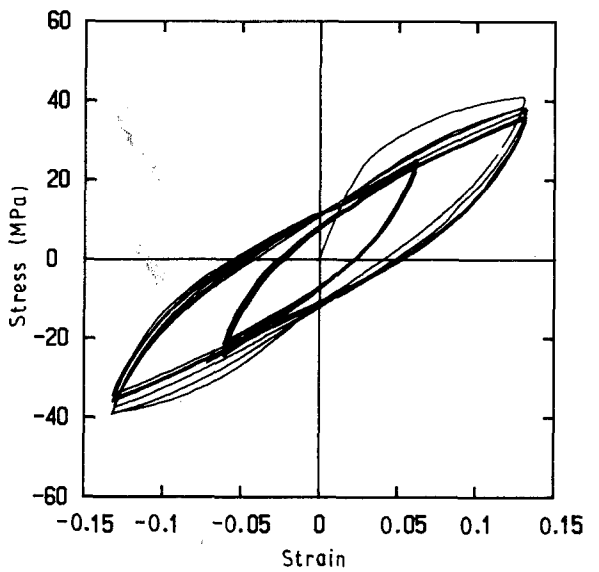

Figure 14 Hysteresis loops at decreasing strain amplitude $\Delta\gamma/2 = 0.13 \rightarrow 0.06$ at a strain rate of $1.8 \times 10^{-3}\,s^{-1}$ under a hydrostatic pressure of 1000 kgf cm^{-2} in PP.

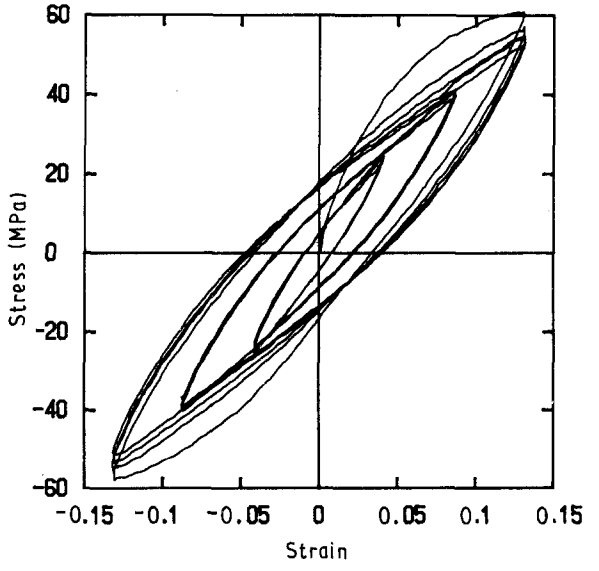

Figure 15 Hysteresis loops at decreasing strain amplitude $\Delta\gamma/2 = 0.13 \rightarrow 0.085 \rightarrow 0.04$ at a strain rate of $1.8 \times 10^{-3}\,s^{-1}$ under a hydrostatic pressure of 1000 kgf cm^{-2} in POM.

In the case of the increasing strain amplitude test, a common feature independent of the test materials will be seen where the new loops obtained after an increase in strain amplitude become similar to those measured at the corresponding strain amplitude as shown in Section 3.1. This may indicate that an increase in strain amplitude erases the memory of the strain histories given in the past.

On the other hand, in the case of the decreasing strain amplitude test, the stress–strain behaviour of PE is different from that of PP and POM. The behaviour of POM is similar to that of PP. For PE, the new loops obtained after a decrease of strain amplitude seem to lie nearly on those at the corresponding amplitude. This may indicate that the stress–strain behaviour of PE is not so affected by the past strain history.

For PP and POM, because the new loops are located inside those at the previous large strain amplitude, their shape is different from the loops at the corresponding strain amplitude, and the stress amplitude is lower than that obtained at the corresponding strain amplitude.

In order to understand the effect of strain history on the stress–strain curve, the test described in Table Ie was conducted. After an increasing strain amplitude (ISA) test between 0.075 and 0.13, the strain amplitude was again changed decreasingly from 0.13–0.075. The hysteresis loops obtained are shown in Figs 16 and 17. For PE, the loops at the decreasing strain amplitude (DSA) test nearly trace over those at the previous corresponding strain amplitude, as if the material forgets the strain histories suffered in the past. For PP, on the other hand, the shape of the loops at DSA is very different from the initial ones. This shows that the stress–strain behaviour for PP is greatly influenced by the past strain histories: the tendency for POM is similar to that for PP. The results for PP and POM obtained at ISA and DSA may be observed for metals such as stainless steels. The results mentioned above are common in the pressure ranges 1–1800 kgf cm^{-2}.

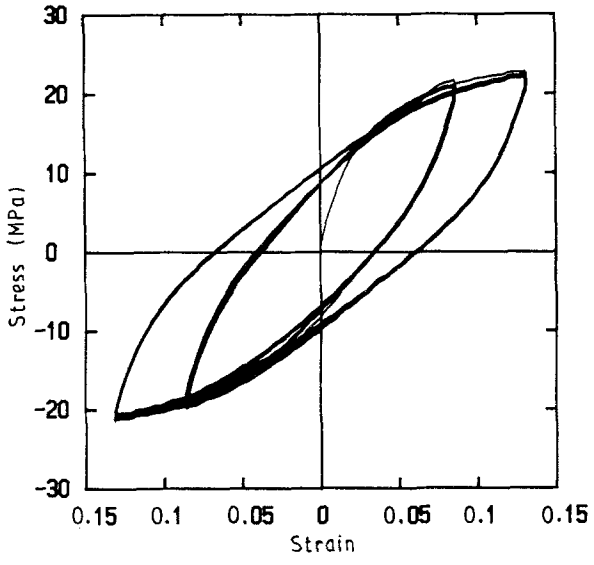

Figure 16 Hysteresis loops at increasing and decreasing strain amplitude $\Delta\gamma/2 = 0.085 \rightarrow 0.13 \rightarrow 0.085 \rightarrow 0.13$ at a strain rate of 1.8×10^{-3} s^{-1} under a hydrostatic pressure of 1000 kgf cm^{-2} in PE.

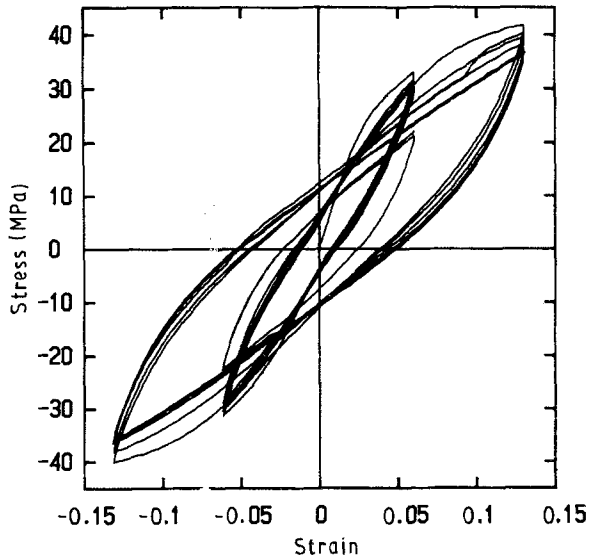

Figure 17 Hysteresis loops at increasing and decreasing strain amplitude $\Delta\gamma/2 = 0.085 \rightarrow 0.13 \rightarrow 0.085$ at a strain rate of 1.8×10^{-3} s^{-1} under a hydrostatic pressure of 1000 kgf cm^{-2} in PP.

4. Conclusion

The cyclic torsional stress–strain behaviour for three kinds of crystalline polymer of PE, PP and POM was studied under hydrostatic pressure up to 2000 kgf cm^{-2} to investigate the effect of cyclic straining on the stress–strain relationship or the constitutive law. Some new curious facts required for constructing the constitutive equation were pointed out: (1) the effect of cyclic straining on the stress–strain relationship is not essentially altered by the hydrostatic pressure; (2) the stress–strain curves after the first strain reversal showed a curious shape which has not been reported to date; (3) the cyclic softening occurred at a fully reversed cyclic loading, while it was not observed at a partly reversed cyclic loading; (4) there were two types of stress–strain behaviour, i.e. PE type where the stress–strain behaviour is not so affected by the strain histories, and PP type where it is very sensitive to the past strain paths.

For the crystalline polymers tested here, as described above, the stress responses associated with strain reversal are very complex. A constitutive law which can explain this curious behaviour has not been proposed on the basis of the micromechanism of polymer chain deformation. As a first step, it may be important to understand why the stress–strain behaviour of PE is very different from that of PP. Future work will be needed.

References

1. M. KITAGAWA and T. MATSUTANI, *J. Mater. Sci.* **23** (1988) 4085.
2. M. KITAGAWA, T. MORI and T. MATSUTANI, *J. Polym. Sci. B* **27** (1989) 85.

3. *Idem, Jpn Soc. Mech. Engng A* **55** (1989) 923.
4. M. KITAGAWA and H. TAKAGI, *J. Mater. Sci.* **25** (1990) 2869.
5. *Idem, J. Polym. Sci. B* **28** (1990) 1943.
6. W. WU and A. P. L. TURNER, *J. Polym. Sci. A* **13** (1975) 1934.
7. K. MATSUSHIGE, E. BAER and S. V. RADCLIFFE, *J. Macromol. Sci. Phys.* **B11** (1975) 565.
8. R. A. DUCKETT and S. H. JOSEPH, *Polymer* **17** (1976) 329.
9. A. A. SILANO, K. D. PAE and J. A. SAUER, *J. Appl. Phys.* **48** (1977) 4076.
10. A. A. SILANO, *Rev. Deform. Behavior Mater.* **4** (1982) 49.
11. S. RABINOWITZ, I. M. WARD and J. S. C. PARRY, *J. Mater. Sci.* **5** (1970) 29.

Received 20 September 1990
and accepted 14 June 1991